International Journal of Power Electronics and Drive Systems (IJPEDS)
Vol. 12, No. 3, September 2021, pp. 1390∼1404
ISSN: 2088-8694, DOI: 10.11591/ijpeds.v12.i3.pp1390-1404

Real time emulator for parallel connected dual-PMSM sensorless control

Khaldoune Sahri[1], Maria Pietrzak-David[2], Lothfi Baghli[3], Abdelaziz Kheloui[4]
[1,4]Laboratoire Commandes des Machines Electriques, Ecole Militaire Polytechnique, 16111 Bordj El Bahri, Algeria
[3]Universite de Tlemcen, LAT, 13000 Tlemcen, Algeria
[2]Université de Toulouse; INPT, UPS, LAPLACE ENSEEIHT, CNRS, 2 rue Charles Camichel, F-31071 Toulouse cedex 7, France

Article Info

Article history:

Received Dec 9, 2019
Revised Mar 30, 2021
Accepted Jul 2, 2021

Keywords:

Emulator
FPGA
Multi-machine system
PMSM
Sensorless control

ABSTRACT

This paper presents a real-time emulator of a dual permanent magnet synchronous motor (PMSM) drive implemented on a field-programmable gate array (FPGA) board for supervision and observation purposes. In order to increase the reliability of the drive, a sensorless speed control method is proposed. This method allows replacing the physical sensor while guaranteeing a satisfactory operation even in faulty conditions. The novelty of the proposed approach consists of an FPGA implementation of an emulator to control the actual system. Hence, this emulator operates in real-time with actual system control in healthy or faulty mode. It gives an observation of the speed rotation in case of fault for the sake of continuity of service. The observation of the rotor position and the speed are achieved using the dSPACE DS52030D digital platform with a digital signal processor (DSP) associated with a Xilinx FPGA.

Corresponding Author:

Khaldoune Sahri
Laboratoire Commandes des Machines Electriques
Ecole Militaire Polytechnique
P.O. Box 17, 16111 Bordj El Bahri, Algeria
Email: khaldoune.sahri@gmail.com

1. INTRODUCTION

Nowadays we can observe very intensive development of AC variable speed and torque drives. Frequently, their topologies use an association of multi-converters and multi-machines systems. These drives operate in several embedded systems such as vehicles, aircraft, ships, trains, and other industrial applications where weight and volume reduction are essential.

To assure the best quality of PMSM vector control, the rotation speed or the rotor position have to be precisely known. Generally, the principal system variables, such as the currents and rotation speed, are measured using physical sensors. To increase reliability and reduce costs, mechanical sensors have to be suppressed. Consequently, the speed information must be reconstituted from measures of electrical quantities using deterministic state observers. Hence, we reconstruct one or several non-measurable or non-accessible system states, in fact, an observer is an estimator which operates in closed loop and has its own dynamics according to the real system. These dynamics are modified by a gain matrix to cancel the estimation error and ensure convergence. To observe the speed and / or position of a PMSM at different speed levels is always a challenge. For PMSM drive two modes of operation must be taken into consideration of course when operating without mechanical sensors [1]-[3]: i) high and medium speed operation, ii) low speed operation.

Using the current measurement and the direct current (DC) bus voltage, various algorithms are used to observe the speed of the machine but they does not show satisfactory fonctionnement in a wide range of speed of the system drive. For example, observers who use the return of the electromagnetic field (EMF) and when the machine is driven with insufficient speed to produce a measurable EMF (low speed), in this case the current sensors cannot detect the position of the rotor which cause a bad observation of the speed [1], [4], [5]. Another point to report is that most estimation and observation algorithms of the speed presented in the literature, use an adjustable model with currents measure. In case of a current sensor fault these algorithms become useless.

In addition, the sensitivity of these observers to the parametric variations [5]-[7], and the static converter dead time (inverter) limits the proper functioning of the observer's and hence the system drive. A dual PMSM system have more degrees of freedom than a single one, (structural actuator and sensors redundancy). So, when a sensor fault appears, a solution that appears very simple is to switch to the actual speed sensor [8]-[10]. The main challenge is to obtain a high dynamic sensorless-drive operation. Taking into account the physical limitations in the real time control of the sensorless synchronous speed drive, we achieve excellent dynamic performances at high and low speeds. The authors interest in this paper, at an experiments of a new control strategy without a speed sensor and without the need to use current sensors it means we observe the rotation speed using the virtual current obtained from the emulator. For a dual PMSM system fed by a dual VSI. We apply an emulator for each machine with its load torque observer and the reference voltages required for the operation of the emulator it means Two individual real time vector controls are applied to drive this global system.

In this way, the obtained deterministic observer replaces the real physical measures, necessary to real-time control system, by corresponding observed variable. Two possibilities exist for working with dSPACE DS52030D digital platform; this emulator function can be implemented on the processor part or on the FPGA target [11]-[13]. To respect its tolerant fault operating two Xilinx FPGA emulators are introduced to increase the system reliability and to admit total physical measure suppression. Certainly, the natural and structural redundancy exists in the DPMSM/DVSI system permitting to switch the speed sensor from first PMSM to second one, or vice versa, when a fault occurs (offset and gain). In the case of current sensor fault its time sharing operation is impossible and it is necessary to dispose three sensors for each PMSM to choose two of them in vector control strategy.

The emulator concept with load torque definition, with "virtual mechanical coupling" in the case of common loads, corresponds to an introduction of analytic redundancy in parallel to real system. In this way the virtual reconstituted variables replace the real physical measures in the control of this system [14]. So, the permanent monitoring detects the sensor failure and generates the decision signal to replace the real measure by corresponding virtual one. The experimental validation of this tolerant sensor fault vector control is made on Laplace DPMSM/DVSI experimental bench and confirms its successful operation and its satisfactory reliability. We present firstly, the different methods for the speed observation that exist in the literature. In the second part, we will put the light on the proposed method which is valid only in the case of a multi-machine system. The studied system is shown in Figure 1.

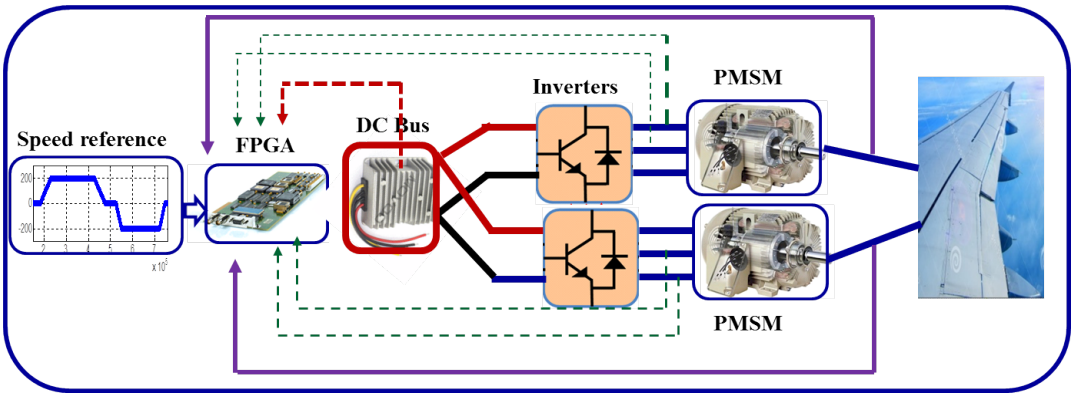

Figure 1. General synopsis of studied system

2. SYSTEM PRESENTATION

2.1. PMSM modelling

The electrical equations expressed in d,q Park frame can be written is being as [15]:

$$\begin{cases} V_d = R_s.I_d + L_s.\dfrac{dI_d}{dt} - \omega_r.L_s.I_q \\ V_q = R_s.I_q + L_s.\dfrac{dI_q}{dt} + \omega_r.L_s.I_d + \omega_r.\phi_f \\ \dfrac{d\omega_r}{dt} = \dfrac{P}{J}.(L_d - L_q).I_d.I_q + \dfrac{P}{J}.\phi_f.I_q - \dfrac{B}{J}.\omega_r - \dfrac{1}{J}.T_L \end{cases} \quad (1)$$

Where I_d and I_q are the direct-axis and quadrature-axis currents (A), V_d, and V_q are the direct-axis and quadrature-axis voltage (V), ω_r is the velocity of the rotor of the motor (rad/s), T_L is the load torque (N-m)
We will investigate the control problem of the PMSM with smooth air gap; we will let $L_d = L_q = L$
In our study we chose a d,q vector control strategy based on a proporsional-integral (PI) cascade control for each PMSM. Thus, the q axis control is made of two loops. The outer loop is the for speed control and the inner loop is for the control of the I_q component. The d axis control has only one loop allowing the direct current regulation I_d.

2.2. State observer

The equations detailed the adjustable model can be rewritten is being as [16]:

$$\begin{cases} (R_s + s.L).\hat{I}_d = \hat{\omega}_r.L.\hat{I}_q + \hat{e}_d + \hat{V}_d + L.l_{11}.\left(I_d - \hat{I}_d\right) + \\ \qquad L.l_{12}.\left(I_q - \hat{I}_q\right) \\ (R_s + s.L).\hat{I}_q = \hat{\omega}_r.L.\hat{I}_d - \hat{e}_q + \hat{V}_q + L.l_{21}.\left(I_d - \hat{I}_d\right) + \\ \qquad L.l_{22}.\left(I_q - \hat{I}_q\right) \\ s.\hat{e}_d = L.l_{31}.\left(I_d - \hat{I}_d\right) \\ s.\hat{e}_q = L.l_{42}.\left(I_q - \hat{I}_q\right) \end{cases} \quad (2)$$

where $\hat{I}_d$ and $\hat{I}_q$ are the direct-axis and quadrature-axis estimated currents (A), $\hat{V}_d$ and $\hat{V}_q$ are the direct-axis and quadrature-axis estimated voltage (V), $\hat{\omega}_r$ is the observed velocity of the rotor of the motor (rad/s).l_{11}, l_{12}, l_{21} ,l_{22}, l_{31} ,l_{42} are adjustable gains used to ensure a good stability of the model. This adjustable model Figure 2 will be used for all the observer versions proposed in this paper such as:

- Rotation speed observation with EMF observation
- Observation of the speed with control of the cross current error.

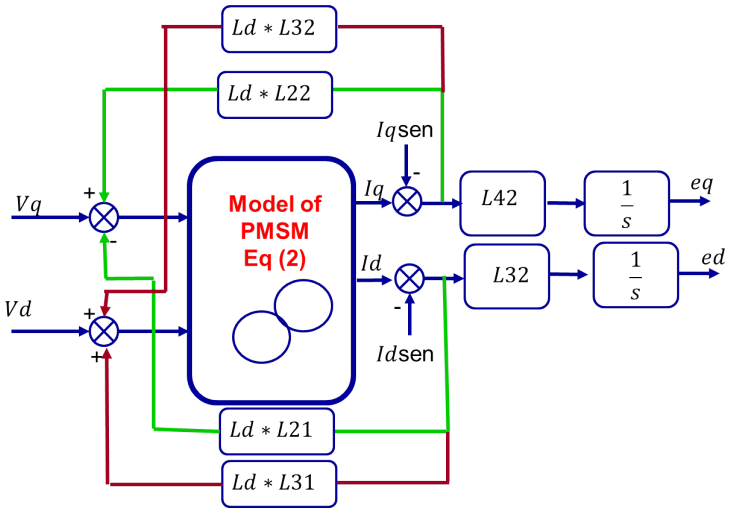

Figure 2. Adjustable model structure

The following section describe the experimental validation of the two method for the observation of the rotation speed of the PMSM.

3. EXPERIMENTAL VALIDATION

The parameters of the PMSM are being as:

- Stator resistance $R_s = 2.281ohms$.
- Direct and quadrature inductance $L_d = 23.173mH$.
- Magnetic Flux $\phi_f = 0.241Wb$.
- Number of pairs of poles $P = 4$.
- PMSM inertia $J = 22,1.10^{-4}kg.m^2$.
- Viscous friction coefficient $f = 1.10^{-4}Nms/rad$.

3.1. Experimental bench

This experimental bench is composed of dual PMSM speed controlled drives fed by dual two level PWM VSIs connected in parallel to DC bus as shown in Figures 3 dan 4. The vector control strategy associated with sinusoidal SVPWM is chosen to control this experimental bench. The implementation is illustrated in Figure 5. The common or separated load torque for each studied PMSM is generated thanks to industrial PMSM controlled torque drives. The torque references are given by the DS1005 processor. In the FPGA target, the following parts have been implemented:

- ADC, DAC and the two incremental encoders.
- Space Vector PWM strategy (SVPWM).
- Direct and reverse transformations 3-phases 123/$\alpha\beta$ and $\alpha\beta$/dq for the two PMSMs .
- Computing the estimated voltages from the duty cycle of pulses and the DC bus voltage.

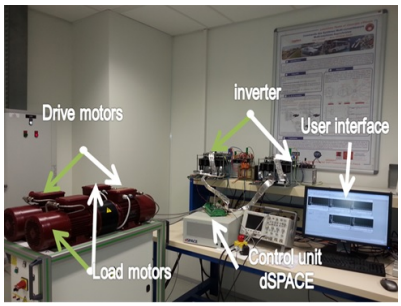

Figure 3. Experimental bench

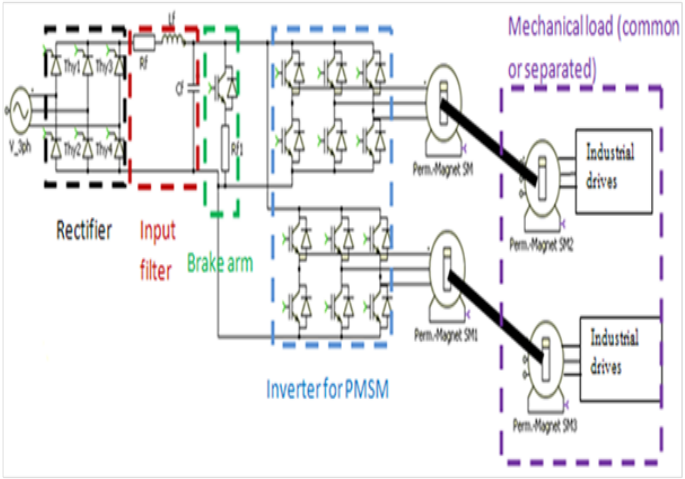

Figure 4. General diagram power part of the experimental bench

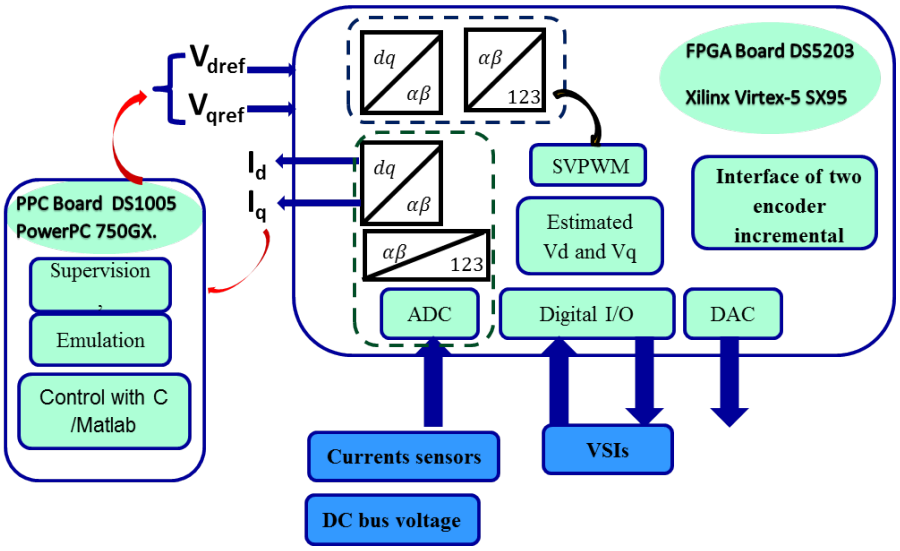

Figure 5. Different control parts implemented in FPGA and PPC card

3.2. Observation of the rotation speed with EMF observer status

The Figure 6 shows the principle of the observation of the rotation speed based on the electromagnetic field (EMF) observer status. The EMF e_d is imposed to zero and this quantity is obtained from the adjustable system model Figure 2. Next, the obtained control error must be linearized to assure a good observation of the rotational speed $\hat{\omega_r}$ [16].

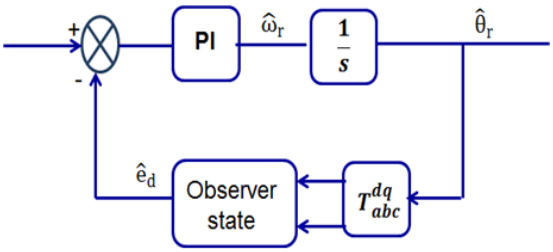

Figure 6. Rotation speed observation with EMF observer status

– Experimental results

In the Figure 7 the rotation speed responses of two M1 and M2 PMSM. The transient and steady state response performances are satisfactory during all speed reference cycles and under different load torques. The responses of dual-PMSM electrical variables, i.e. Id, Iq, Vd, and Vq , are presented in Figures 8 and 9.

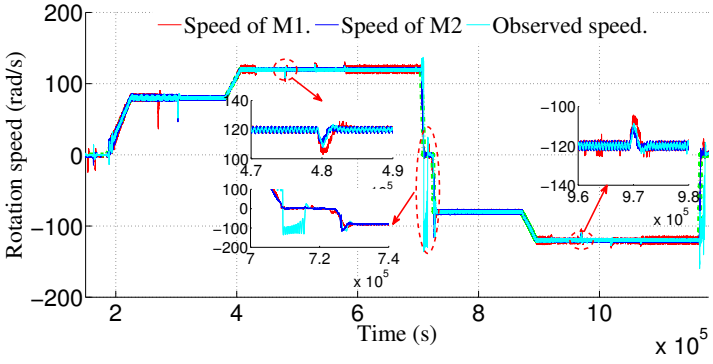

Figure 7. Rotation speed control

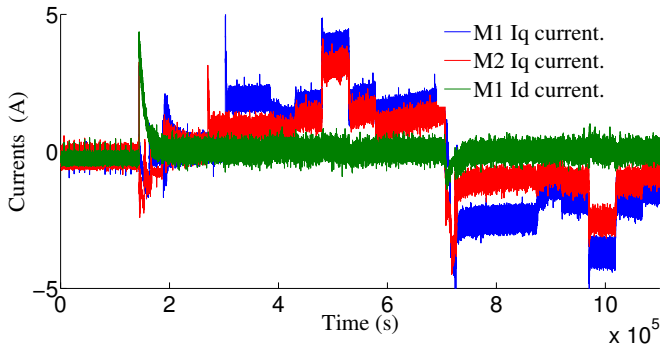

Figure 8. Current Id and Iq responses

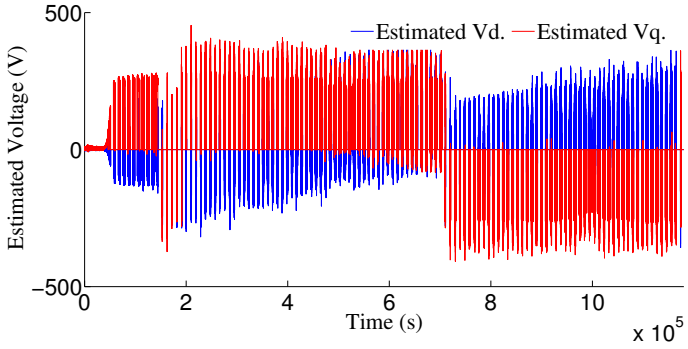

Figure 9. Estimated voltages Vd and Vq

3.3. Observation of the speed control by controlling the cross currents error (analytical redundancy)

We can observe the position or the speed thanks to a PI controller using the crossed error between the measured and the estimated currents Figure 10. The principle of this observer is given in the Figure 10. The error is obtained by evaluating:

$$(I_{qest}.I_d - I_{dest}.I_q) - (I_{qest} - I_q).\frac{\phi_f}{L} \tag{3}$$

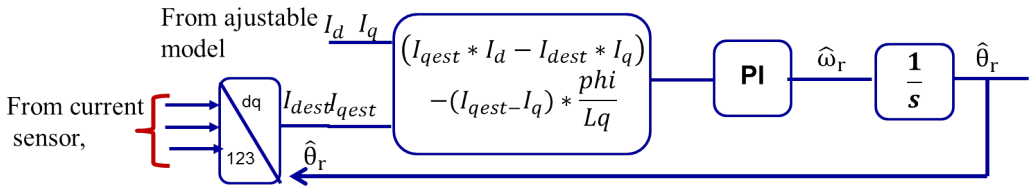

Figure 10. Rotation speed estimation with regulation of error cross currents

A robust and stable correction can be based on approach MRAS synthesized using through Popov's hyper stability criteria [17], [18].

– Experimental results

We analyze the PMSM system behavior with the same rotation speed reference cycles. So, the speed responses of M1 and M2 PMSMs are satisfactory during all reference cycles, small oscillations are observed in the steady state after load torque application as shown in Figures 11 and 12. The actual and observed mechanical positions of PMSM are shown in the Figure 13. We notice the effective precision in both rotation directions. In order to test the robustness of the Dual PMSM speed observation, both velocity and load profile

were applied using the different proposed methods. For a wide operation range (low, medium and high speed), these algorithms are not satisfying. To address this issue, each algorithm must be used in one speed range. EMF based observers are not used at low speed because of the low EMF and are better in medium and high speed. Observation of the speed by controlling the cross currents error, is used for low and medium speed range. Several others approaches are used for speed estimation. These methods require huge memory and involve high computational complexity and memory storage [15], [19].

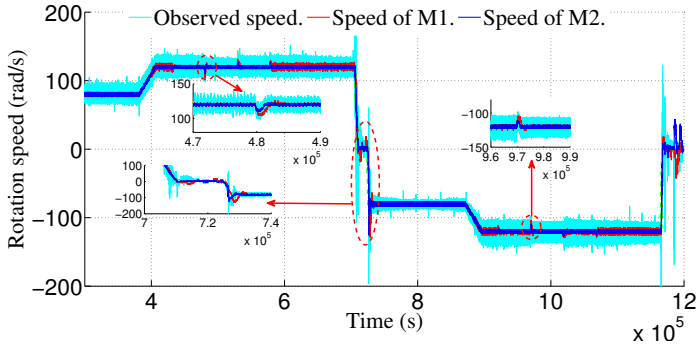

Figure 11. Rotation speed control

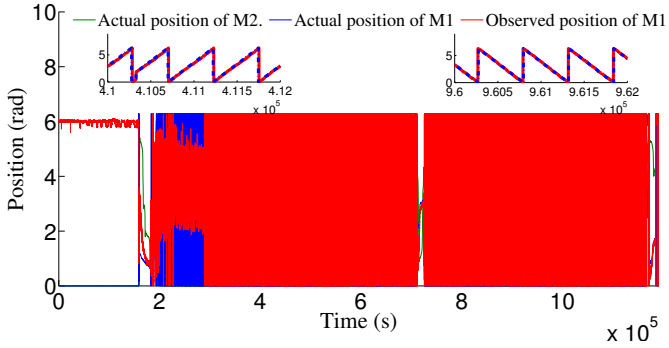

Figure 12. Actual and observed position

3.4. Natural structural redundancy

In the Dual PMSM system, there is a natural physical redundancy, because each machine has the mechanical or electrical sensors to achieve a closed loop control. This redundancy will be called structural with natural redundancy. The principle of this method is explained on the following figure: The Figure 13 show the proper functioning of the system with physical speed sensor, and when fault sensor operation occurs, we can continue satisfactory operating with only one speed sensor shared by the two machine to achieve a closed loop control with satisfactory operation.

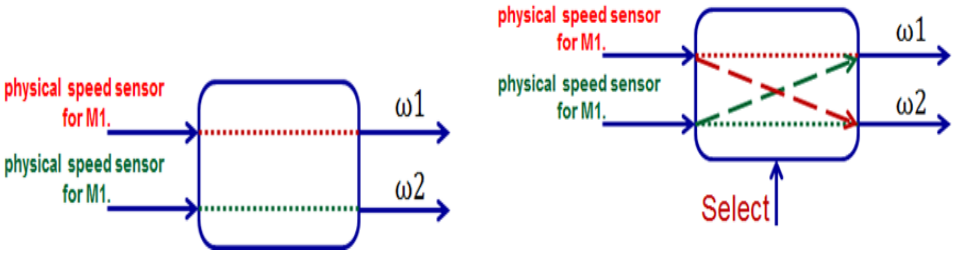

Figure 13. Fonctionnement of Dual PMSM with physical sensors

The following method was adopted in order to validate our idea. The state of the signal select change in function of fault in speed sensor . Without fault; the signal select takes the value of zero and when we have fault in the first sensor the signal select passes to 1, then it passes to 2 when we have fault in the second sensor (Figure 14). In our case the decision on faulty speed sensor if the sensor give a value of 80% for the reference speed. For the decisional organ the following algorithms has been implemented:

$$select = \begin{cases} 1 & \text{if speed M1 ¡ 80 \% of ref speed.} \\ 2 & \text{if speed M1 ¡ 80 \% of ref speed.} \end{cases}$$

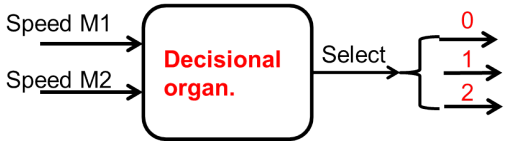

Figure 14. Decision device

– Experimental results

As shown in the Figures 15 and 16, we start the operation with the physical speed sensors that is to say that the system has not yet suffered a defect, then a defect is caused, in our case it is indeed a defect in the second sensor of Speed of the second motor and then we continuing the operation of the system with a single speed sensor shared for the closed loop vector control of the two motors. It should be noted that the natural switching between the physical sensor does not allow the system to be started (it is not possible to start with one speed sensor).

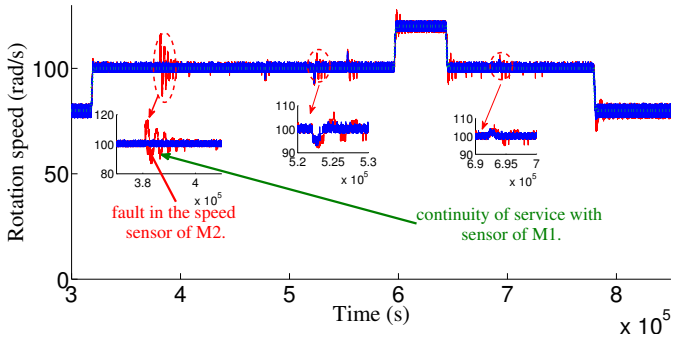

Figure 15. Rotation speed control

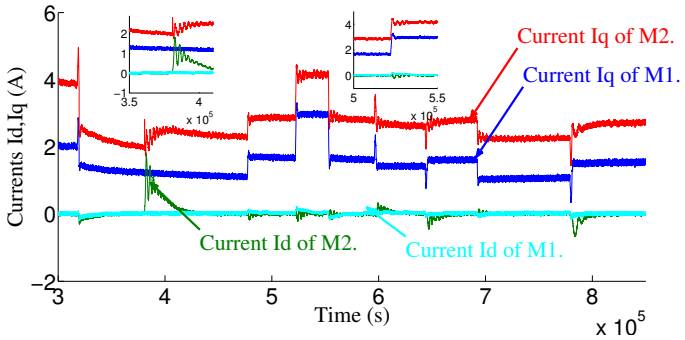

Figure 16. Currents Id and Iq

4. THE PROPOSED SENSELESS SPEED FOR THE SYSTEM

We describe in this section the design, implementation, and experimental validation of a real-time hardware-in-the-loop emulation of a dual PMSM. The PMSM machine are modelled using a flexible piecewise linear state space approach [20]; and are simulated in hard real-time with 10 ns time step, which enables high-fidelity modelling of PMSM dynamics. We validate the real-time PMSM drive emulator by making real-time comparisons with a reference hardware model of a PMSM drive. The validation of this real-time DPMSM emulator is made by real-time comparison with a reference hardware model of a DPMSM drive. In this way we want analyze experimentally the operation of the HIL-DPMSM drive emulation under different operating scenarios, in health and faulty conditions. Therefore we experimentally demonstrate the capability of the hardware in the loop PMSM drive emulation under various operating scenarios, including fault conditions [21]-[23].

The implementation of the different control configurations is done using the dSPACE DS52030D digital platform containing a PowerPC DS1005 and a Xilinx FPGA DS5203. The task dispatching between PPC and FPFA can be modified during the final optimized final implementation of global DPMSM drive system and also its load in common or separated configurations. The computing time on the FPGA processor is 10 ns. Thus, we can use the implementation of the continuous mathematical model of the PMSM directly on the FPGA Target. The computing time on the PPC DS1005 is 100 μs. So the mathematical model of the PMSM should be discretized.

In the FPGA target, the following parts have been implemented Figure 17:

- PWM, ADC, DAC and the two incremental encoders.
- Modulation (PWM).
- d,q /$\alpha\beta$ transformations for the two PMSM.
- 123 /$\alpha\beta$ and $\alpha\beta$/d,q transformations for the two PMSM.
- Mathematical model of the PMSM in this way a more complex PMSM model can be implemented on FPGA target.

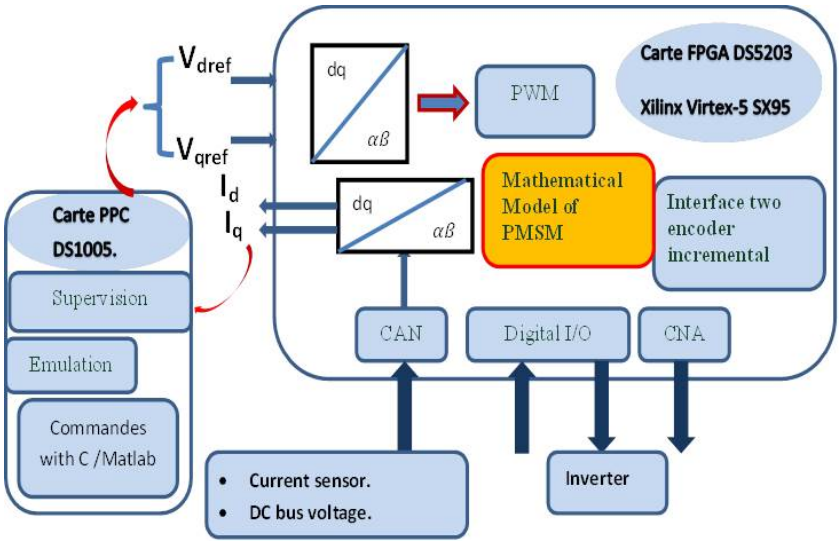

Figure 17. Different parts of real time control implemented in FPGA and PPC card

All the parts implemented are resumed in Figure 17. The mathematical model of the PMSM Figures 18 requires Luenberger observer to reconstruct the torque load. For the supply voltages Vd and Vq necessary for the proper functioning of the emulator, it can be obtained from the references voltages of the actual system. We can obtain them using the DC bus voltage and the pulses of the inverters [24]:

$$V_{dq} = [d]_{dq} V_{dc}$$

$$I_{dq} = \frac{3}{2}[d]_{dq} I_{dc}$$

$$d_d.V_{dc} = V_d$$

$$d_q.V_{dc} = V_q$$

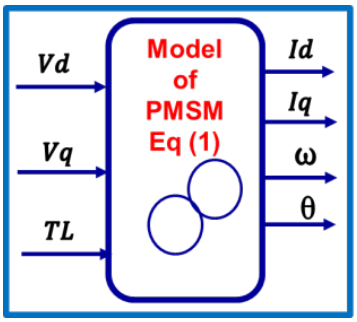

Figure 18. The mathematical model of the PMSM

d: is the matrix of control. Unfortunately, if we have a fault in physical sensors the references voltage calculated by this method becomes instable and we do not have enough time to replace the faulty sensor by the emulator variables. To fix this problem, the reference voltages are obtained by a closed loop vector control of the mathematical model implemented on FPGA or PPC in Figure 19. So the voltage are calculated in closed loop and we obtain a robust and reliable observer. For the torque load TL it can be observed by the following algorithm (Figure 20).

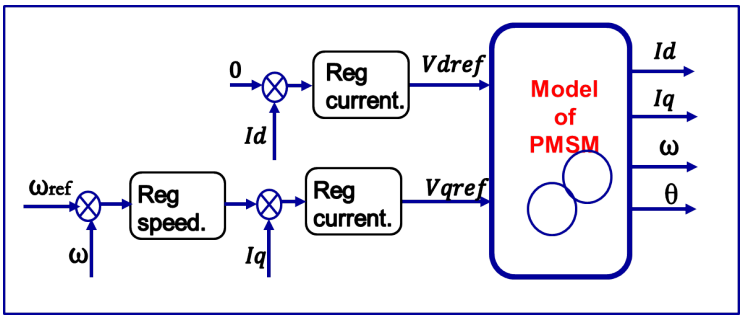

Figure 19. Closed loop vector control of the mathematical model

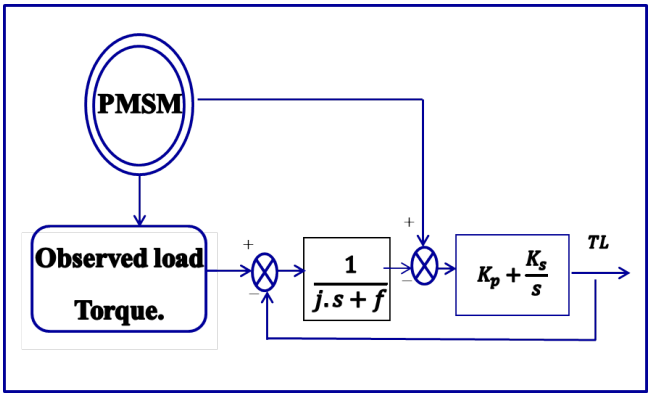

Figure 20. Observed torque load

– Experimental results

The model of the PMSM machine is implemented on the FPGA target in order to validate it, in real time conditions. Firstly, the laws are used for the controls implemented on the card PPC DS1005, PWM, and calibration of inputs/outputs. The results presented in Figures 21-24 allow the comparison of the measurable variables (stator currents and speed) of the PMSM, with the ones of the model running, in real time, on the FPGA. This approach validates the proper functioning of the model, the parameter identification and the vector control of the machine. Next, this model is implemented in the FPGA, in order to use the emulated model for the control of the actual system.We validated the real-time emulation by making steady state and transient operation comparisons with the actual PMSM .

Additionally, we demonstrate the ability of the real-time PMSM emulation, as a hardware in the loop prototyping platform, to control the actual system in a wide speed range; from low to high speed. The key advantages of the proposed the real-time emulation platform are twofold. First, the piecewise linear state space modelling approach enables comprehensive modelling of PMSM, including the dynamics that occur on the control [25], [26]. Second, the flexible modelling implementation enables the platform to be used as a powerful tool for rapid prototyping and validation [8]. In the next section, we will present the results obtained during a fault in the speed sensor, the observed torque variable must be reconstructed from the healthy machine as shown in Figures 25-28.

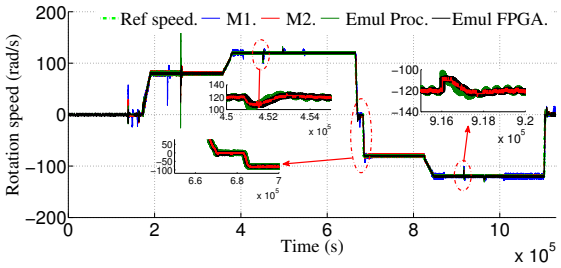

Figure 21. Comparison of actual and emulated speed

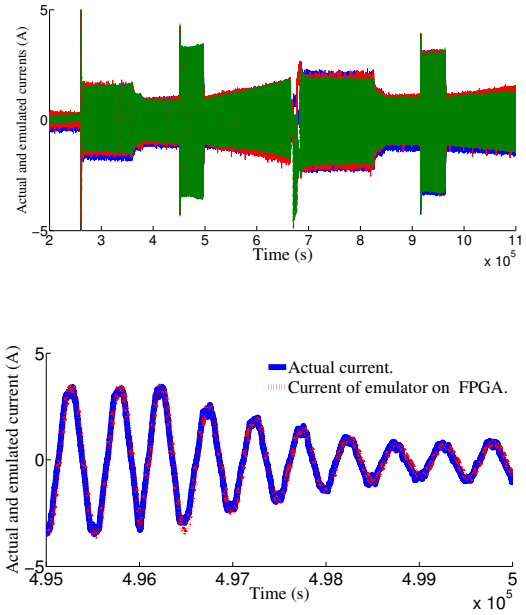

Figure 22. Actual current of the PMSM and their emulators

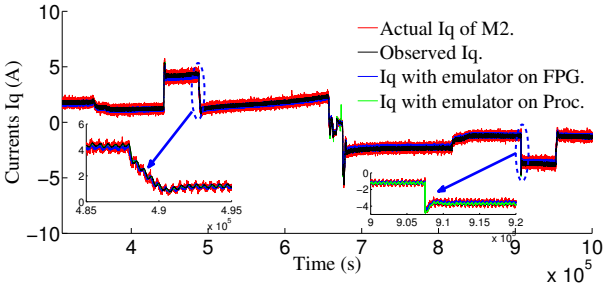

Figure 23. Actual currents Iq of the PMSM and their emulator

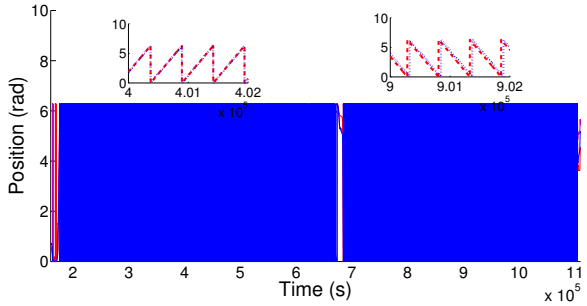

Figure 24. Emulated and actual position

– Experimental results
– Using the emulator FPGA as observer

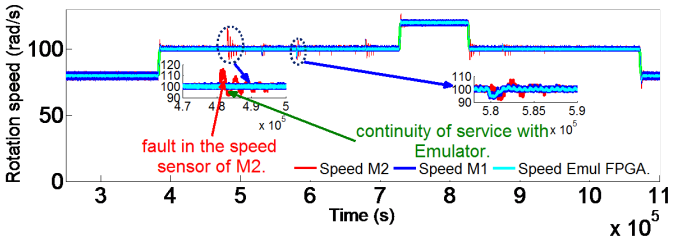

Figure 25. Rotation speed control

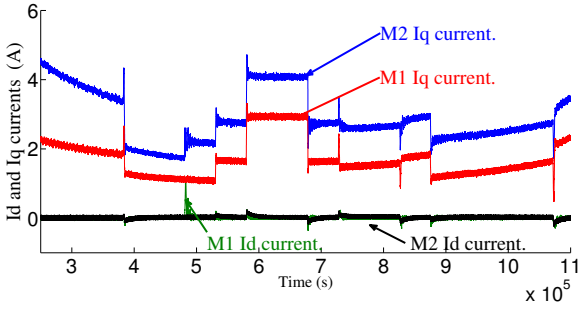

Figure 26. Iq and Id currents

– Using the emulator PPC as the observer

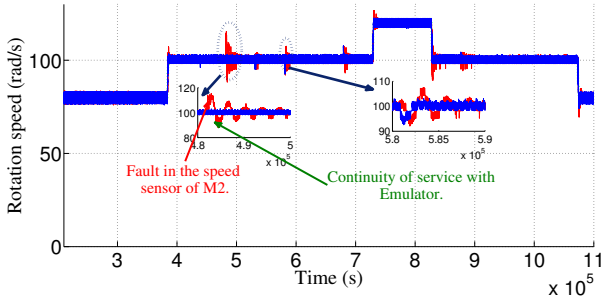

Figure 27. Rotation speed control

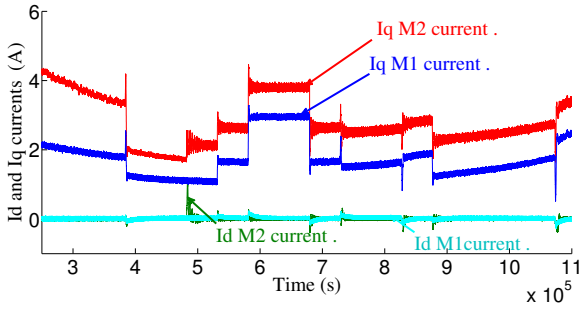

Figure 28. Iq and Id currents

The results obtained shows clearly that the mathematical model of the machine replaces accurately the physical speed sensor. So, when we impose the rotation speed cycle for this DPMSM we observe good performances of real rotation speeds controlled with emulated one. The load torque modification don't modify the system precision, the zooms shown in the Figures 16-18 proves the satisfying behavior of this DPMSM system.

The results show that it is possible to continue the operation of the system in the case of a current sensor fault, because the currents Id and Iq required for the vector control can be obtained directly from the emulator which is implemented on the FPGA or the PPC. The results obtained also show that the emulator can be used for the diagnosis and detection of the various existing mechanical fault by the use of the different method of frequency analysis. It means that we can used the emulated mathematical model as a reference system and when we have a mechanical fault, we can easily see this fault in the actual currents by comparing with the emulated currents . Consequently, we can easily conclude on the nature of fault.

The Figure 29 as shown presents a comparison between the reconstitution of speed on FPGA and processor. The results of comparison show that the implemented emulator on the FPGA or the PPC has the same dynamics; so we can distribute the tasks efficiently on FPGA and processor. Therefore, the resources of FPGA can be minimized in a very effective way.

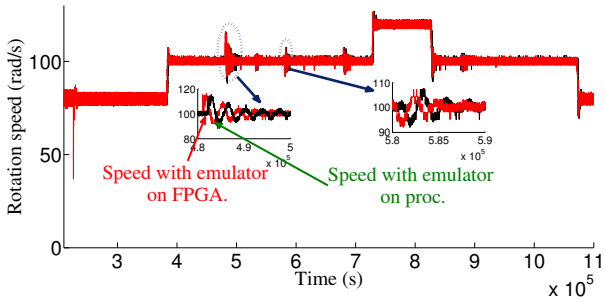

Figure 29. Emulated speed

5. CONCLUSION

FPGA is used for the control of two PMSMs with operation at variable speeds and variable torque loads. The objective of this work is to validate the performance of the real time dual-PMSM drive by using the vector control law. We compare the reference system (which is the actual physical system) with the emulated system implemented on FPGA and on the PPC. We also demonstrate the ability of the Hardware-in-the loop emulation in real time to control the real system under fault of speed sensor conditions and we will demonstrate also other faulty condition for example by injecting open phase fault, and current sensor fault in the emulator drive system. In fact, this emulator can be considered as an adjustable model that does not use gains to adjust the mathematical model; but it uses much more the observation of the load torque as parameter for the adjustment of the model contrary to the existing methods in the literature.

ACKNOWLEDGEMENT

We thank all those who contributed to make this work, including my supervisors in the EMP school and the LAPLACE laboratory in toulouse University and all my friends for their support.

REFERENCES

[1] A. S. Budden, R. Wrobel, D. Holliday, P. Mellor, and P. Sangha," Sensorless control of permanent magnet machine drives for aerospace applications," *2005 International Conference on Power Electronics and Drives Systems*, 2005, pp. 372-377, doi: 10.1109/PEDS.2005.1619715.

[2] T. Mueller, P. Thiemann, C. See, A. Ghani, and A. Bati,"Direct flux control–a sensorless control method of pmsm for all speeds–basics and constraints," *Electronics Letters*, vol 53, no. 16, pp. 1110-1111, 2005, doi: 10.1049/el.2017.1772.

[3] J.-S. Hu, D. Yin, and Y. Hori," Fault-tolerant traction control of electric vehicles," *Control Engineering Practice*, vol. 19, no. 2, pp. 204–213, February 2011, doi: 10.1016/j.conengprac.2010.11.012.

[4] B. Gerard, S. Caux, and P. Maussion," Redundant Position Observer Improvement for Sensorless PMSM at Low Speed," *2006 IEEE International Symposium on Industrial Electronics*, 2006, pp. 2083-2088, doi: 10.1109/ISIE.2006.295894.

[5] Z. Song, Z. Hou, C. Jiang, and X. Wei," Sensorless control of surface permanent magnet synchronous motor using a new method," *Energy Conversion and Management*, vol. 47, no. 15, pp. 2451–2460, September 2006, doi: 10.1016/j.enconman.2005.11.009.

[6] B. Akin, S. B. Ozturk, H. A. Toliyat, and M. Rayner," DSP-Based Sensorless Electric Motor Fault-Diagnosis Tools for Electric and Hybrid Electric Vehicle Powertrain Applications," in *IEEE Transactions on Vehicular Technology*, vol. 58, no. 6, pp. 2679-2688, July 2009, doi: 10.1109/TVT.2009.2012430.

[7] M. E. H. Benbouzid, D. Diallo, and M. Zeraoulia," Advanced Fault-Tolerant Control of Induction-Motor Drives for EV/HEV Traction Applications: From Conventional to Modern and Intelligent Control Techniques," in *IEEE Transactions on Vehicular Technology*, vol. 56, no. 2, pp. 519-528, March 2007, doi: 10.1109/TVT.2006.889579.

[8] S. Bolognani, M. Zordan, and M. Zigliotto," Experimental fault-tolerant control of a pmsm drive," in *IEEE Transactions on Industrial Electronics*, vol. 47, no. 5, pp. 1134-1141, Oct. 2000, doi: 10.1109/41.873223.

[9] R. L. de Araujo Ribeiro, C. B. Jacobina, E. R. C. Da Silva, and A. M. N. Lima," Fault-tolerant voltage-fed PWM inverter AC motor drive systems," in *IEEE Transactions on Industrial Electronics*, vol. 51, no. 2, pp. 439-446, April 2004, doi: 10.1109/TIE.2004.825284.

[10] D. Bidart, M. Pietrzak-David, P. Maussion, and M. Fadel," Mono inverter dual parallel PMSM-structure and control strategy," *2008 34th Annual Conference of IEEE Industrial Electronics*, 2008, pp. 268-273, doi: 10.1109/IECON.2008.4757964.

[11] C. B. Jacobina, R. L. de Araujo Ribeiro, A. N. Lima, and E. C. Da Silva," Fault-tolerant reversible AC motor drive system," in *IEEE Transactions on Industry Applications*, vol. 39, no. 4, pp. 1077-1084, July-August 2003, doi: 10.1109/TIA.2003.814567.

[12] T.-H. Liu, J.-R. Fu, and T. A. Lipo," A strategy for improving reliability of field-oriented controlled induction motor drives," in *IEEE Transactions on Industry Applications*, vol. 29, no. 5, pp. 910-918, Sept.-Oct. 1993, doi: 10.1109/28.245714.

[13] O. Wallmark, L. Harnefors, and O. Carlson," Control Algorithms for a Fault-Tolerant PMSM Drive," in *IEEE Transactions on Industrial Electronics*, vol. 54, no. 4, pp. 1973-1980, Aug. 2007, doi: 10.1109/TIE.2007.895076.

[14] R. R. Errabelli and P. Mutschler," Fault-Tolerant Voltage Source Inverter for Permanent Magnet Drives,"in *IEEE Transactions on Power Electronics*, vol. 27, no. 2, pp. 500-508, Feb. 2012, doi: 10.1109/TPEL.2011.2135866.

[15] S. Maiti, C. Chakraborty, and S. Sengupta," Simulation studies on model reference adaptive controller based speed

estimation technique for the vector controlled permanent magnet synchronous motor drive," *Simulation Modelling Practice and Theory*, vol. 17, no. 4, pp. 585–596, April 2009, doi: 10.1016/j.simpat.2008.08.017.

[16] R. P. Burgos, P. Kshirsagar, A. Lidozzi, F. Wang, and D. Boroyevich," Mathematical Model and Control Design for Sensorless Vector Control of Permanent Magnet Synchronous Machines," *2006 IEEE Workshops on Computers in Power Electronics*, 2006, pp. 76-82, doi: 10.1109/COMPEL.2006.305655.

[17] W. Sae-Kok, D. Grant, and B. Williams," System reconfiguration under open-switch faults in a doubly fed induction machine," *IET Renewable Power Generation*, vol. 4, no. 5, pp. 458–470, September 2010, doi: 10.1049/iet-rpg.2010.0005.

[18] A. M. Mendes and A. M. Cardoso," Fault-Tolerant Operating Strategies Applied to Three-Phase Induction-Motor Drives,"in *IEEE Transactions on Industrial Electronics*, vol. 53, no. 6, pp. 1807-1817, Dec. 2006, doi: 10.1109/TIE.2006.885137.

[19] D. Campos-Delgado, D. Espinoza-Trejo, and E. Palacios," Fault-tolerant control in variable speed drives: a survey," *IET Electric Power Applications*, vol. 2, no. 2, pp. 121–134, March 2008, doi: 10.1049/iet-epa:20070203.

[20] J. Poon, E. Chai, I. Čelanović, A. Genić, and E. Adzic," High-fidelity real-time hardware-in-the-loop emulation of PMSM inverter drives," *2013 IEEE Energy Conversion Congress and Exposition*, 2013, pp. 1754-1758, doi: 10.1109/ECCE.2013.6646919.

[21] F. Alvarez-Gonzalez, A. Griffo, B. Sen, and J. Wang," Real-Time Hardware-in-the-Loop Simulation of Permanent-Magnet Synchronous Motor Drives Under Stator Faults," in *IEEE Transactions on Industrial Electronics*, vol. 64, no. 9, pp. 6960-6969, Sept. 2017, doi: 10.1109/TIE.2017.2688969.

[22] Q.-T. An, L.-Z. Sun, K. Zhao, and L. Sun," Switching function model-based fast-diagnostic method of open-switch faults in inverters without sensors,"in *IEEE Transactions on Power Electronics*, vol. 26, no. 1, pp. 119-126, Jan. 2011, doi: 10.1109/TPEL.2010.2052472.

[23] F. Zidani, D. Diallo, M. E. H. Benbouzid, and R. Naït-Saïd," A Fuzzy-Based Approach for the Diagnosis of Fault Modes in a Voltage-Fed PWM Inverter Induction Motor Drive," in *IEEE Transactions on Industrial Electronics*, vol. 55, no. 2, pp. 586-593, Feb. 2008, doi: 10.1109/TIE.2007.911951.

[24] C.-C. Yeh and N. A. Demerdash," Induction Motor-Drive Systems with Fault Tolerant Inverter-Motor Capabilities," *2007 IEEE International Electric Machines Drives Conference*, 2007, pp. 1451-1458, doi: 10.1109/IEMDC.2007.383642.

[25] M. Karpenko and N. Sepehri, "Hardware-in-the-loop simulator for research on fault tolerant control of electrohydraulic actuators in a flight control application," *Mechatronics*, vol. 19, no. 7, pp. 1067– 1077, October 2009, doi: 10.1016/j.mechatronics.2009.01.008.

[26] R. D. Turney, C. Dick, D. B. Parlour, J. Hwang," Modeling and implementation of dsp fpga solutions," in *Proceedings of International Conference on Signal Processing Applications and Technology (ICSPAT)*, 1999, pp. 1–4.